Electronic Supplementary Material (ESI) for Dalton Transactions.
This journal is © The Royal Society of Chemistry 2017

Electronic Supplementary Information

Metal-ion induced ferromagnetic polarization in mixed-spin system

Li Yang,[1] Jing Li,[1] Tian-Cheng Pu,[2] Ming Kong,[1] You Song*[1]

[1] State Key Laboratory of Coordinate Chemistry, Collaborative Innovation Center of Advanced Microstructures, School of Chemistry and Chemical Engineering, Nanjing University, Nanjing 210093, China. [2] Department of Chemical and Biomolecular Engineering, John Hopkins University, Baltimore, Maryland 21218, United States. Correspondence and requests for materials should be addressed to Y.S. (email: yousong@nju.edu.cn)

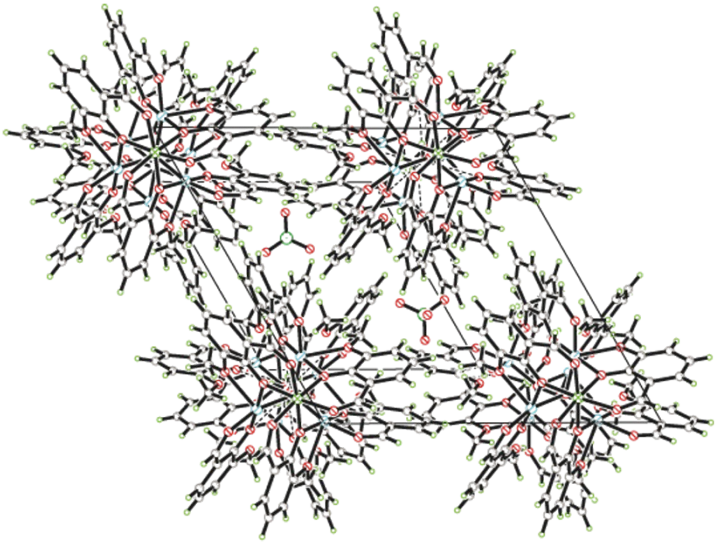

Figure S1. The stacking diagram of complexes **1-3**, as viewed along axis *b*.

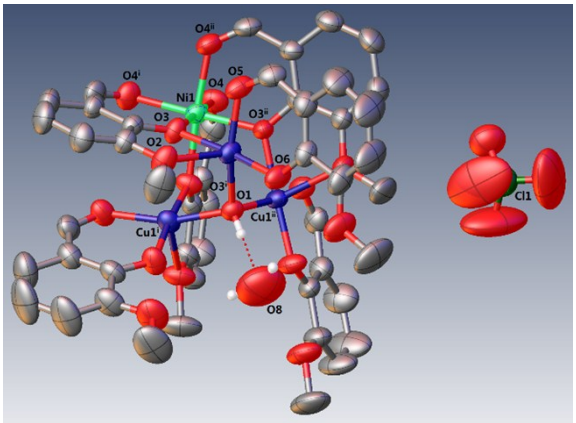

Figure S2. Molecular structure of complex **2**. The hydrogen atoms of the ligands are omitted.

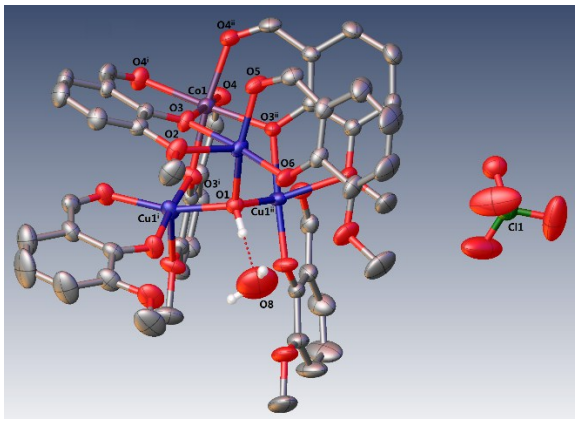

Figure S3. Molecular structure of complex **3**, the hydrogen atoms of the ligands are omitted.

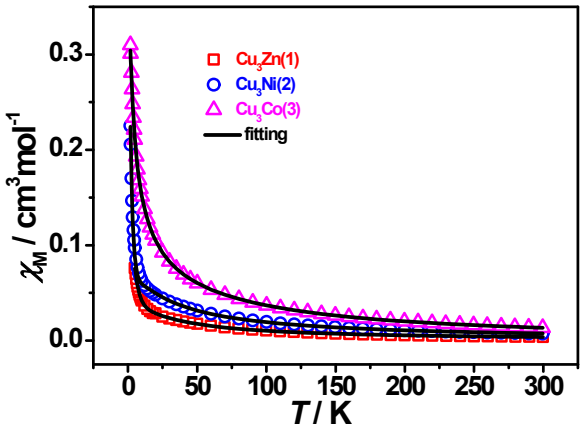

Figure S4. Temperature dependence of the magnetic susceptibility in the form of χ_M and in 2 kOe for **1**–**3**. The solid lines represent the best fit with the *PHI* program.

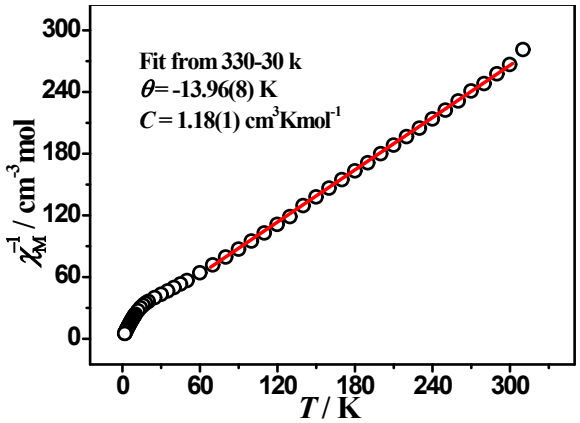

Figure S5. Plot of χ_M^{-1} *vs T* for **1**. The solid line represents the best−fit curve following Curie-Weiss law.

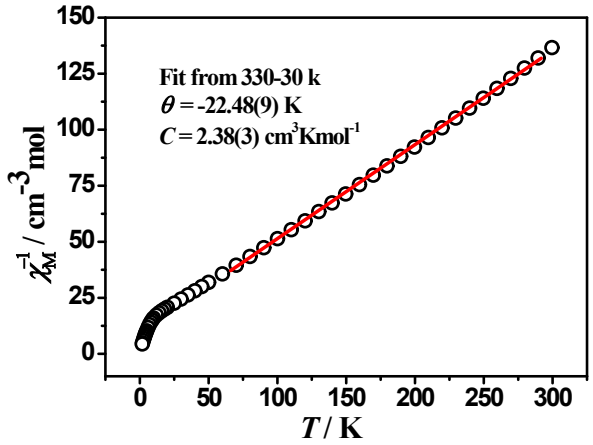

Figure S6. Plot of χ_M^{-1} *vs T* for **2**. The solid line represents the best−fit curve following Curie-Weiss law.

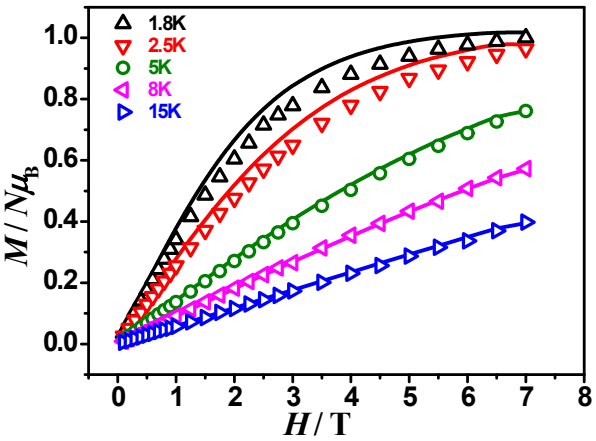

Figure S7. Plot of *M vs H* for **1** at the indicated temperatures. The solid lines are the best-fit curves by spin approximation and combined fitting process with susceptibility.

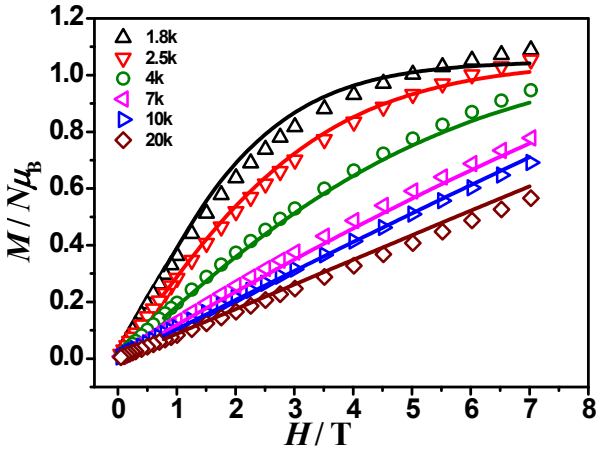

Figure S8. Plot of *M vs H* for **2** at the indicated temperatures. The solid lines represents the best−fit curves.

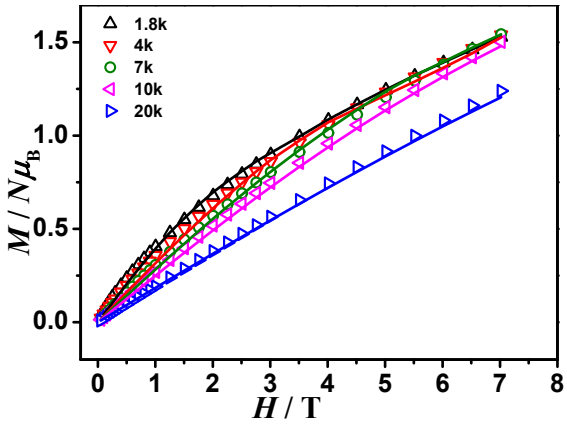

Figure S9. Plot of *M vs H* for **3** at the indicated temperatures. The solid lines are the best-fit curves.

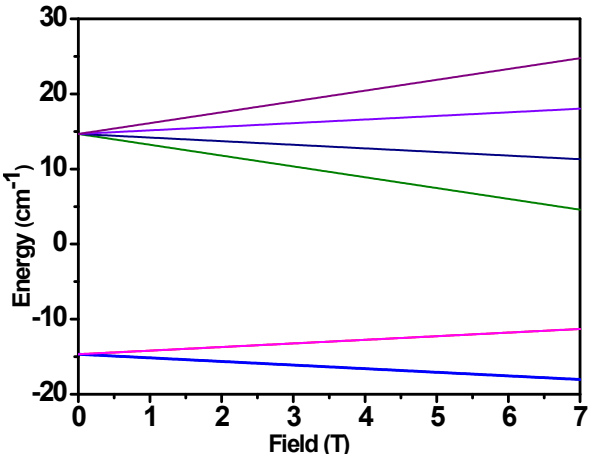

Figure S10. Plot of low-lying Zeeman energy levels for **1** using a full calculation.

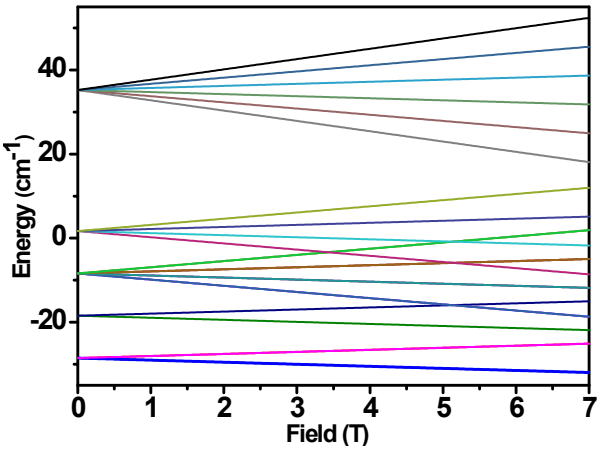

Figure S11. Plot of low-lying Zeeman energy levels for **2** using a full calculation

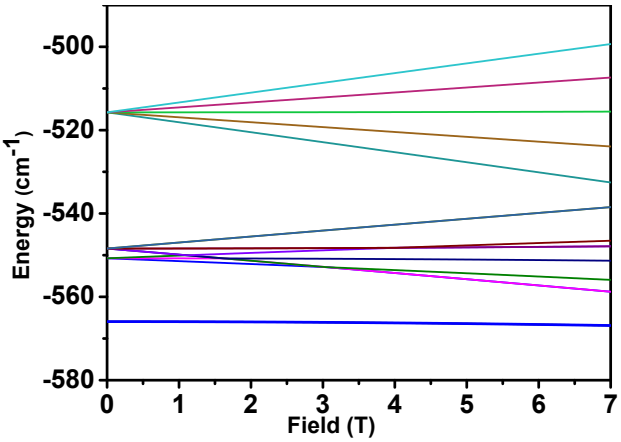

Figure S12. Plot of low-lying Zeeman energy levels for **3** using a full calculation. Considering the clarity of the graph, only the ground state, first excited state and second excited state were been shown.

Table S1. Metal–Ligand Bond Lengths (Å) and Angles (°) in Complex **1**.

Cu1–O1	1. 9710(19)	Cu1–O6	1.888(3)	Zn1–O4	2.084(3)
Cu1–O2	2.288(3)	Zn1–O3	2.074(3)	Zn1–O4^{i}	2.084(3)
Cu1–O3	2.011(3)	Zn1–O3^{i}	2.074(3)	Zn1–O4^{ii}	2.084(3)
Cu1–O5	1.947(3)	Zn1–O3^{ii}	2.074(3)	O8–H8A	0.8484
O1–Cu1^{ii}	1. 9710(19)	O1–Cu1^{i}	1.966(2)	O3^{ii}–Zn1–O4^{ii}	86.25(12)
O3–Cu1–O2	74.47(11)	O6–Cu1–O5	93.70(13)	O4–Zn1–O4^{ii}	88.60(14)
O1–Cu1–O2	105.41(10)	O3–Zn1–O3^{i}	87.10(11)	O3–Zn1–O4^{i}	170.87(13)
O5–Cu1–O2	91.91(14)	O3–Zn1–O3^{ii}	87.10(11)	O3^{i}–Zn1–O4^{i}	86.25(12)
O6–Cu1–O2	100.87(13)	O3^{i}–Zn1–O3^{ii}	87.10(11)	O3^{ii}–Zn1–O4^{i}	86.25(12)
O1–Cu1–O3	88.18(13)	O3–Zn1–O4	86.25(12)	O4–Zn1–O4^{i}	88.60(14)
O5–Cu1–O3	89.98(12)	O3^{i}–Zn1–O4	98.79(14)	O4^{ii}–Zn1–O4^{i}	88.60(14)
O6–Cu1–O3	174.18(14)	O3^{ii}–Zn1–O4	170.87(12)	Cu1^{i}–O1–Cu1	108.43(12)
O5–Cu1–O1	161.38(13)	O3–Zn1–O4^{ii}	98.79(13)	Cu1^{i}–O1–Cu1^{ii}	108.43(12)
O6–Cu1–O1	89.75(15)	O3^{i}–Zn1–O4^{ii}	170.87(13)	Cu1–O1–Cu1^{ii}	108.43(12)

Symmetry codes: (i) −x+y, −x+1, z; (ii) −y+1, x−y+1, z.

Table S2. Metal–Ligand Bond Lengths (Å) and Angles (°) in Complex **2**.

Cu1–O1	1.9679(13)	Cu1–O6	1.876(2)	Ni1–O4	2.027(2)
Cu1–O2	2.291(2)	Ni1–O3	2.026(2)	Ni1–O4^{i}	2.027(2)
Cu1–O3	2.000(2)	Ni1–O3^{i}	2.026(2)	Ni1–O4^{ii}	2.027(2)
Cu1–O5	1.941(2)	Ni1–O3^{ii}	2.026(2)	O3^{ii}–Ni1–O4^{ii}	89.10(9)
Cu1^{i}–O1	1.9679(13)	Cu1^{ii}–O1	1.9679(13)	O4–Ni1–O4^{ii}	88.69(10)
O3–Cu1–O2	74.55(8)	O6–Cu1–O5	93.63(10)	O3–Ni1–O4^{i}	175.37(9)
O1–Cu1–O2	105.71(8)	O3–Ni1–O3^{i}	87.05(9)	O3^{i}–Ni1–O4^{i}	89.11(9)
O5–Cu1–O2	90.96(10)	O3–Ni1–O3^{ii}	87.05(9)	O4^{ii}–Ni1–O4^{i}	95.33(10)
O6–Cu1–O2	101.48(10)	O3^{i}–Ni1–O3^{ii}	87.05(9)	O4–Ni1–O4^{i}	88.69(10)
O1–Cu1–O3	87.93(10)	O3–Ni1–O4	89.10(9)	O4^{ii}–Ni1–O4^{i}	88.68(10)
O5–Cu1–O3	89.84(9)	O3^{i}–Ni1–O4	95.33(10)	Cu1^{i}–O4–Cu1	108.32(10)
O6–Cu1–O3	174.79(10)	O3^{ii}–Ni1–O4	175.37(9)	Cu1^{i}–O4–Cu1^{ii}	108.32(10)
O5–Cu1–O1	161.90(10)	O3–Ni1–O4^{ii}	95.33(10)	Cu1–O4–Cu1^{ii}	108.31(10)
O6–Cu1–O1	89.96(11)	O4^{i}–Ni1–O4^{ii}	88.69(10)		

Symmetry codes: (i) −x+y, −x+1, z; (ii) −y+1, x−y+1, z.

Table S3. Metal–Ligand Bond Lengths (Å) and Angles (°) in Complex **3**.

Cu1–O1	1.9590(14)	Cu1–O6	1.877(2)	Co1–O3	2.062(2)
Cu1–O2	2.274(2)	Co1–O4	2.062(2)	Co1–O3^{i}	2.062(2)
Cu1–O3	1.997(2)	Co1–O4^{i}	2.062(2)	Co1–O3^{ii}	2.062(2)
Cu1–O5	1.942(2)	Co1–O4^{ii}	2.062(2)	O3^{ii}–Co1–O4	97.93(10)
Cu1^{i}–O1	1.9590(14)	Cu1^{ii}–O1	1.9590(14)	O3–Co1–O4^{ii}	87.44(9)
O3–Cu1–O2	74.70(9)	O6–Cu1–O5	94.02(10)	O3^{i}–Co1–O4^{ii}	97.93(10)
O1–Cu1–O2	105.49(8)	O4–Co1–O4^{i}	88.46(10)	O3^{ii}–Co1–O4^{ii}	172.31(9)
O5–Cu1–O2	91.78(10)	O4^{ii}–Co1–O4^{i}	88.46(10)	O3^{i}–Co1–O3	86.68(9)
O6–Cu1–O2	101.26(10)	O3–Co1–O4^{i}	97.93(10)	O3^{ii}–Co1–O3	86.68(9)
O1–Cu1–O3	88.49(11)	O3^{i}–Co1–O4^{i}	172.31(9)	O3^{ii}–Co1–O3^{i}	86.68(9)
O5–Cu1–O3	89.64(9)	O3^{ii}–Co1–O4^{i}	87.44(9)	Cu1^{i}–O4–Cu1	108.28(11)
O6–Cu1–O3	174.66(11)	O4^{ii}–Co1–O4	88.46(10)	Cu1^{i}–O4–Cu1^{ii}	108.28(11)
O5–Cu1–O1	161.46(10)	O3–Co1–O4	172.31(9)	Cu1–O4–Cu1^{ii}	108.28(11)
O6–Cu1–O1	89.26(12)	O3^{i}–Co1–O4	87.44(9)		

Symmetry codes: (i) −x+y, −x+1, z; (ii) −y+1, x−y+1, z.